

Aerosol Synthesis of Spherical Morphology Boron Nitride Powders from Organoborate Precursors

Gary L. Wood,[†] Jerzy F. Janik,[‡] Eugene A. Pruss,[§] Dirk Dreissig,[§] William J. Kroenke,[§] Tassilo Habereeder,[§] Heinrich Nöth,^{||} and Robert T. Paine*[§]

Departments of Chemistry and Chemical Engineering and the University of New Mexico/National Science Foundation Center for Micro-engineered Materials, University of New Mexico, Albuquerque, New Mexico 87131, Department of Chemistry, Valdosta State University, Valdosta, Georgia 31698, AGH University of Science and Technology, Faculty of Fuels and Energy, Al. Mickiewicza 30, 30-059 Krakow, Poland, and Department of Chemistry, University of Munich, Butenandstrasse 5-B, Haus D, D-81377 Munich, Germany

Received September 9, 2005. Revised Manuscript Received December 15, 2005

The reaction of aerosol droplets of the organoborate reagent (MeO)₃B, suspended in nitrogen, with gaseous ammonia in a flight tube heated to 800–1500 °C was used to produce, in high yield, spherical morphology precursor powders BN_xO_yC_z that contain decreasing amounts of oxygen and carbon as the process temperature and mole fraction of ammonia increased. Subsequent static nitridation of the precursor powder under ammonia gave spherical morphology BN powders with low (<1 wt %) oxygen and carbon contents. The powders were characterized by elemental analysis, DRIFT-IR, XRD, SEM, and TEM methods. A weak molecular complex (MeO)₃B·NH₃ has been previously reported to exist, and this species was isolated and structurally characterized by single-crystal X-ray diffraction methods. Aerosol conversions using (MeO)₃B/MeOH, H₃BO₃/MeOH, and B₂O₃/MeOH solutions were also examined, and the results are briefly described.

Introduction

Hexagonal boron nitride (h-BN) is a commercially produced refractory ceramic powder that enjoys large-scale use in the fabrication of crucibles, electrical insulators, and mold-release liners.^{1,2} Furthermore, its novel combination of physical and chemical properties has led to smaller scale applications as a component in cosmetic formulations and in filled organic polymer composites for thermal management materials.^{3,4} Recently, BN has also been examined as a selective gas sorbent⁵ and a hydrogen storage medium.^{6–9} In the commercial setting, h-BN powders are typically prepared in large, metallurgical-type syntheses that employ readily available starting materials such as boric acid and melamine or urea. Boric acid is the preferred boron source due to its low cost and facile thermal dehydration chemistry.

The resulting powders have a platelet primary particle morphology with varying degrees of agglomeration and oxygen contents ranging from 4 to 0.3 wt % depending upon the specific processing protocol used in manufacturing. As interest in new applications grows for this carbon-like material, so do efforts to discover alternative particle morphologies with modified performance characteristics. The spherical BN particle morphology is one that is of particular interest since, for example, monodispersed and polydispersed spheres should produce higher particle packing fractions for BN-filled organic polymer composites.³

The first report of the formation of spherical BN particles appeared in 1990 in a European patent.¹⁰ It was claimed that under low-temperature CVD conditions the reaction of BCl₃ and NH₃ produced a spherical powder; however, few characterization details were provided. In 1991 we reported an aerosol-assisted vapor-phase synthesis (AAVS) employing liquid ammonia solutions of poly(borazinylamine) that produced smooth, spherical BN particles with an average diameter of 1 μm.¹¹ Subsequent nitridations of the smooth spheres led to the formation of multifaceted particles that retained the general spherical shape and size of the initially formed material. Unfortunately, the expense and difficulty of polymer precursor preparation hindered further development of these particles. However, industrial interest in the form encouraged us to seek alternative starting reagents. In 2000 we reported an aerosol synthesis using saturated (0.9 M) aqueous solutions of H₃BO₃ as the starting material, and

* To whom correspondence should be addressed. E-mail: rtpaine@unm.edu.

[†] Valdosta State University.

[‡] AGH University of Science and Technology.

[§] University of New Mexico.

^{||} University of Munich.

- (1) Paine, R. T.; Narula, C. K. *Chem. Rev.* **1990**, *90*, 73.
- (2) Haubner, R.; Wilhelm, M.; Weissenbacker, R.; Lux, B. *Struct. Bonding* **2002**, *102*, 2.
- (3) Paine, R. T.; Pruss, E. A.; Wood, G. L.; Schwierkowski, C.; Hill, R. F.; Chapelle, C.; Kroenke, W. J. *ACS Symp. Ser.* **2002**, *804*, 27.
- (4) Hill, R. F.; Supancic, P. H. *J. Am. Ceram. Soc.* **2002**, *85*, 851.
- (5) Janik, J. F.; Ackerman, W. C.; Paine, R. T.; Hua, D. W.; Maskara, A.; Smith, D. M. *Langmuir* **1994**, *10*, 514.
- (6) Ma, R.; Bando, Y.; Zhu, H.; Sato, T.; Xu, C.; Wu, D. *J. Am. Chem. Soc.* **2002**, *124*, 7672.
- (7) Tang, C.; Bando, Y.; Ding, X.; Qi, S.; Golberg, D. *J. Am. Chem. Soc.* **2002**, *124*, 14550.
- (8) Ma, R.; Golberg, D.; Bando, Y.; Sasaki, T. *Philos. Trans. R. Soc. London Ser. A* **2004**, *362*, 2161.
- (9) Oku, T.; Kuno, M.; Narita, I. *J. Phys. Chem. Solids* **2004**, *65*, 549.

(10) Iltis, A.; Maguier, C. Eur. Patent 396,448, July 11, 1990.

(11) Lindquist, D. A.; Kodas, T. T.; Smith, D. M.; Xiu, X.; Hietala, S. L.; Paine, R. T. *J. Am. Ceram. Soc.* **1991**, *74*, 3126.

the aerosol droplets were allowed to react with gaseous ammonia in a heated (1000–1200 °C) flight tube.^{12,13} The short residence time of the aerosol in the reaction zone resulted in incomplete nitridation with formation of intermediate boron oxynitride compositions, BN_xO_y , having relatively high oxygen contents (37–55 wt %). The particles displayed a smooth, spherical morphology with an average particle diameter of $\sim 1 \mu\text{m}$. Subsequent calcinations of the particles under NH_3 gave h-BN particles that retained low levels of oxygen (1–4 wt %). Depending upon specific nitridation conditions, the particle morphology remained spherical with a smooth or bladed surface.

Although the boric-acid-based aerosol process is practical for the preparation of gram quantities of spherical morphology BN particles, it still suffers from several drawbacks. These include the following: (a) large amounts of water from the aqueous boric acid solution are swept from the aerosol generator into the heated aerosol reactor flight tube; (b) dehydration of H_3BO_3 produces additional water in the hot zone; (c) water vaporization is endothermic, and steam dilutes the ammonia injected into the hot zone which in turn reduces the degree of B_2O_3 nitridation; (d) steam back-reacts with partially nitrided BN_xO_y material; (e) the resulting BN_xO_y particles harvested at the end of the hot zone have high weight percent oxygen contents; (f) the large amount of oxygen in the BN_xO_y particles is slowly replaced during the second-stage static nitridation; (g) there is significant mass loss during the nitridation. These factors led us to continue to investigate additional aerosol precursor systems. For example, the aerosol conversion of aqueous solutions of guanidinium tetraborate, pentaborate, and nonaborate¹⁴ resulted in improved production rates due to slightly higher effective boron concentrations in the aerosol streams. However, oxygen contents in the intermediate BN_xO_y particles still remained relatively high (23–38 wt %). Due to these results, solventless or nonaqueous-based aerosol precursor chemical systems have been sought.

There are few readily available, inexpensive boron reagents that are significantly soluble in nonaqueous solvents appropriate for aerosol formation and even fewer liquid boron compounds that could be employed directly to generate a boron-rich aerosol stream. However, commercially available trialkylborates, $(\text{RO})_3\text{B}$ ($\text{R} = \text{Me}, \text{Et}, \text{Pr}, \text{Bu}$), are low-viscosity, molecular liquids at 23 °C that offer the potential to serve as aerosol precursors. We report here on the successful use of $(\text{MeO})_3\text{B}$, in neat form and in methanol solution, as an aerosol precursor for the formation of spherical morphology BN particles.^{15,16} In addition, the use of methanol solutions of H_3BO_3 and B_2O_3 as aerosol precursors is briefly described.

Experimental Section

Materials. Organoborates, boric acid, and boric anhydride were purchased from Aldrich Chemical Co., and anhydrous ammonia was obtained from Air Products. Methanol was purchased from VWR.

Preparation of the Complex, $(\text{MeO})_3\text{B}\cdot\text{NH}_3$. A sample of $(\text{MeO})_3\text{B}$ (1.04 g, 10 mmol) was loaded into a Schlenk tube under dry nitrogen, and the tube was cooled to $-196 \text{ }^\circ\text{C}$ and evacuated. Dry NH_3 (10 mmol), measured by gas volume, was condensed onto the borate, and the mixture was warmed to 23 °C. A white solid formed immediately that readily sublimed in vacuo at 45 °C. Single crystals of the adduct were obtained by sublimation. Anal. Calcd for $\text{C}_3\text{H}_{12}\text{BNO}_3$: C, 29.80; H, 9.93; B, 8.95; N, 11.59. Found: C, 21.32; H, 9.38; B, 9.59; N, 10.86. MS (CI with isobutane) (*m/e*, ion, rel inten): 177 ($\text{M} + \text{C}_4\text{H}_8^+$) 65, 176 ($\text{M} + \text{C}_4\text{H}_7^+$) 33, 122 ($\text{M} + \text{H}^+$) 37, 121 (M^+) 10, 90 ($\text{C}_2\text{H}_5\text{BNO}_2^+$) 100. IR (KBr, cm^{-1}): 3393 (ν_{NH}), 3198 (ν_{NH}), 1630, 1402 (ν_{BN}), 1319 (ν_{BO}), 1060 (ν_{CO}), 930, 704.

Preparation of the Powders. Aerosol syntheses were performed as described previously.^{12–14} The aerosol flight tube consisted of a mullite tube (3.5 in. \times 60 in.) fitted with gastight stainless steel end caps. The tube was placed in a horizontal three-zone Lindberg tube furnace (model 54779). The entrance to the reactor was connected to the top of a glass sample container (4.5 cm \times 23 cm) by use of Tygon tubing. The bottom of the sample container was closed with a thin polyethylene cap. A sidearm on the container wall allowed for periodic introduction of additional liquid $(\text{MeO})_3\text{B}$ reagent during the preparation. The exit end of the reactor tube was connected through a short section of Teflon tubing to an impact filter or a bag filter. An aerosol mist of $(\text{MeO})_3\text{B}$ or $(\text{MeO})_3\text{B}/\text{MeOH}$ was produced by placing the polyethylene-capped sample container over an ultrasonic transducer operated at 1.7 kHz. The mist was swept with a controlled nitrogen gas stream (0.5–3.0 L/min) into the furnace via inlets passing through the entrance end cap.

Characterization of the Powders. The aerosol-generated powders and calcined powders were compositionally analyzed for oxygen (Advanced Ceramics Corp. and St. Gobain/Carborundum) and B, N, C, and H (INEOS and Galbraith Laboratories). In addition, powders were examined by TGA (Perkin-Elmer TGA7), diffuse reflectance (DRIFT) IR (Mattson Galaxy 2020), powder X-ray diffraction (Siemens D5000), scanning electron microscopy (SEM Hitachi S-800), and transmission electron microscopy (TEM, JEOL JEM 2010, 200 keV). Densities were determined by He pycnometry and surface areas by multipoint BET methods. Single-crystal X-ray diffraction analysis was performed on a Siemens P4 diffractometer with an area detector and low-temperature device operating at 193 K. A single crystal was mounted in perfluoropolyether oil. $\text{Mo K}\alpha$ radiation ($\lambda = 0.71073 \text{ \AA}$) was used with a graphite single-crystal monochromator. Pertinent data collection and refinement information are summarized in Table 1. Data were collected in the hemisphere mode with a measurement rate of 10 s per frame. No extinction correction was applied, and the absorption correction employed SADABS. Data reduction was accomplished by use of SAINT (Siemens Analytical Instruments). The structure was solved by direct methods and refined using full-matrix least-squares techniques (SHELXS-97) based on F^2 . All non-hydrogen atoms were refined anisotropically. Hydrogen atoms were located in difference maps and refined.

Results and Discussion

Although there are several approaches available for producing aerosol streams of chemical reagents, the aerosol

(12) Pruss, E. A.; Wood, G. L.; Kroenke, W. J.; Paine, R. T. *Chem. Mater.* **2000**, *12*, 19.

(13) Paine, R. T.; Kroenke, W. J.; Pruss, E. A. U.S. Patent 6,348,179 B1, Feb. 19, 2002.

(14) Wood, G. L.; Janik, J. F.; Visi, M. Z.; Schubert, D. M.; Paine, R. T. *Chem. Mater.* **2005**, *17*, 1855.

(15) The original disclosure of this work appears in "Organoboron Route and Process for Preparation of Boron Nitride", U.S. Patent filing April 23, 2002.

(16) Paine, R. T.; Kroenke, W. J.; Pruss, E. A.; Wood, G. L.; Janik, J. F. U.S. Patent 6,824,753 B2, Nov 30, 2004.

Table 1. Summary of Crystallographic Data and Data Collection Parameters

mol formula	C ₃ H ₁₃ BN ₂ O ₃
fw	135.96
cryst syst	tetragonal
space group	I4(1)/a
a/Å	19.519(5)
b/Å	19.519(5)
c/Å	7.712(3)
V/Å ³	2938.1(14)
Z	16
D _c /g cm ⁻³	1.229
μ/mm ⁻¹	0.101
cryst size/mm	0.10 × 0.10 × 0.20
index range	-24 ≤ h ≤ 24 -24 ≤ k ≤ 19 -10 ≤ l ≤ 10
2θ	58.42
reflins collected	8175
reflins unique	1598
reflins obsd (4σ)	1090
GOOF	1.032
R ₁ [I > 4σ(I)]	0.0491
wR ₂	0.1181

generator in this study utilizes a piezoelectric transducer to impart energy to overcome the surface tension of the liquid reagent or its solution. Hence, a first test of the utility of a reagent as an aerosol precursor involves determining its response to ultrasonic agitation. We find that pure (MeO)₃B, (EtO)₃B, (n-PrO)₃B, and (n-BuO)₃B, MeOH solutions of each as well as MeOH solutions of B₂O₃ and H₃BO₃, provide aerosols that are transported, in a stream of nitrogen gas, into the reactor hot zone. Each of the (RO)₃B reagents is reported to be thermally stable to at least 350 °C,¹⁷ and (MeO)₃B is said to be stable to 470 °C.¹⁸ Such stability should favor the occurrence of intermolecular elimination chemistry between NH₃ and borates over decomposition of the (RO)₃B molecules without nitridation.

The reactivity of trialkoxy boranes toward various Lewis bases has been examined to a limited extent.¹⁷ Pertinent to this study, it appears that (MeO)₃B and (EtO)₃B form weak 1:1 adducts with several organoamines and ammonia.^{17,19} Perhaps the first report on the combination of (MeO)₃B and NH₃ appeared in a U.S. Patent filing by Schechter,²⁰ who claimed the formation of an adduct (MeO)₃B·NH₃ in flowing gas streams of reagents and in azeotropic mixtures of reagents. The adduct was described as a colorless, crystalline solid that sublimed at 45 °C. It was also noted that the adduct thermally decomposed with formation of unidentified boron–nitrogen compounds. Soon thereafter, Goubeau^{21–23} reported on the reactions of (MeO)₃B with NH₃ and organoamines. It was noted that (MeO)₃B and NH₃ combined between -50 and 23 °C to produce (MeO)₃B·NH₃ as a colorless, crystalline solid. It was further stated that the adduct decomposed between 30 and 300 °C with formation of MeOH, Me₂O, and mixtures of numerous solid compounds characterized only by partial elemental analyses. It was proposed that boron

nitride was an ultimate end product in some decomposition pathways.

Indeed, despite the apparent thermal stability of organoborates, the use of (MeO)₃B as a boron precursor for BN synthesis has been described in two early patents.^{24,25} May and Levasheff²⁴ claimed that when equimolar amounts of (MeO)₃B and NH₃ vapors were passed through a hot zone maintained at 500 °C, a crystalline product was obtained that gave elemental analysis values (wt %) of B 9.35, N 10.75, H 6.2, C 17.2, and O (by difference) 56.5. These data may be compared with calculated values for the adduct (MeO)₃B·NH₃ (C₃H₁₂BNO₃): B, 8.95; N, 11.59; H, 9.93; C, 29.80; O, 39.73. When the hot zone was held at 850 °C, white fluffy solids were obtained with compositions that vary with the rate at which the reactants were swept through the hot zone. The composition (wt %) ranges were B 27–32, N 26–34, H 2.5–3.0, C 0.7–1.0, and O (by difference) 30–44. Although BN may be formed under these conditions, the solids retain significant amounts of oxygen and the nitridation reaction is incomplete under the conditions reported. Bienert and co-workers²⁵ claimed formation of detrition-resistant BN pressed bodies using boron–nitrogen–hydrogen compounds of general formula BN_{3-x}H_{6-3x}. Curiously, the examples provided in the patent²⁵ described the formation of such precursors from the reaction of (MeO)₃B and NH₃ for which there is no evidence of the formation of an oxygen-free precursor. These incomplete reports encouraged us to reexamine the molecular chemistry between (MeO)₃B and NH₃ and attempt to utilize these reagents in an aerosol-assisted vapor-phase synthesis of spherical BN particles. During the course of our studies, Bando and co-workers²⁶ reported on the use of (MeO)₃B/MeOH/NH₃ mixtures in a CVD synthesis of BN. They noted formation of a B–N–O precursor solid at 700 °C that, following further nitridation under NH₃ at 1100 °C, gave spherical BN particles (*d* = 50–400 nm). As will be described below, this process closely relates to our aerosol synthesis.

In our studies of the molecular chemistry, mixtures of (MeO)₃B and NH₃, in 1:1, 1:2, and 1:4 mole ratios, were prepared by combining the reagents at -196 °C and allowing the reagents to mix at 23 °C. In each case, a white solid formed. The 1:1 compound was fully characterized, and the 1:2 and 1:4 combinations gave the 1:1 compound with additional ammonia partially adsorbed to the solid. Further evidence for the adsorption of excess NH₃ on the 1:1 compound was found in qualitative tensimetric titrations with NH₃. The excess ammonia was reversibly desorbed during sublimation as evidenced by “hopping” of the solids and pressure build up in the sublimator. The 1:1 compound completely sublimes at 45 °C, forming colorless crystals on cool surfaces. The unusual nature of the 1:1 compound was further revealed in our attempts to characterize samples. All attempts to obtain satisfactory elemental analyses (C, H, B, N) were unsuccessful. It became evident that this is a result of the strong tendency of the complex to partially dissociate

(17) Steinberg, H. *Organoboron Chemistry*; J. Wiley: New York, 1964; Vol. 1, Chapter 4. Lappert, M. F. *Chem. Rev.* **1956**, *56*, 959.

(18) Makishima, S.; Yoneda, Y.; Tajima, T. *J. Phys. Chem.* **1957**, *61*, 1618.

(19) Urs, S. V.; Gould, E. S. *J. Am. Chem. Soc.* **1952**, *74*, 2948.

(20) Schechter, W. H. U.S. Patent 2,629,732, Feb 24, 1953.

(21) Goubeau, J.; Boehm, U. *Z. Anorg. Allg. Chem.* **1951**, *266*, 161.

(22) Goubeau, J.; Link, R. *Z. Anorg. Allg. Chem.* **1951**, *267*, 27.

(23) Goubeau, J.; Ekhoff, E. *Z. Anorg. Allg. Chem.* **1952**, *268*, 145.

(24) May, F. H.; Levasheff, V. V. U.S. Patent 2,824,787, Feb 25, 1958.

(25) Bienert, K.; Lang, W.; Weidner, H. U.S. Patent 3,711,594, Jan 16, 1973.

(26) Tang, C.; Bando, Y.; Golberg, D. *Chem. Commun.* **2002**, 2826.

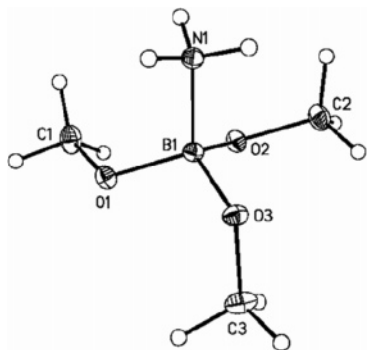


Figure 1. Molecular structure and atom-labeling scheme for $(\text{MeO})_3\text{B}\cdot\text{NH}_3$.

even at 23 °C, and static sublimation at 45 °C is accompanied by some dissociation. The precarious stability of the complex is further indicated by attempts to obtain ^1H and ^{11}B NMR spectra in CDCl_3 . In a patent, Sallay²⁷ reported a ^1H NMR spectrum [$^1\text{H}(\text{CDCl}_3)$ δ 3.50 (OCH₃), 1.45 (NH)] for a material suggested to be the 1:1 complex; however, we have been unable to replicate the spectrum.²⁸ Instead, we observe that in an open NMR tube NH_3 is rapidly evolved from the 1:1 complex upon contact with CDCl_3 while in a sealed tube gas bubbles form upon contact of solute and solvent. NMR spectra (^1H , ^{11}B) of the resulting solutions obtained at 23 and -45 °C show only a resonance assigned to base-free $(\text{MeO})_3\text{B}$. An infrared spectrum for the 1:1 compound in a KBr pellet shows absorptions that can be assigned to NH, BN, BO, and CO stretching modes. This spectrum differs significantly from the spectrum reported by Sallay obtained from a Nujol mull,^{27,28} and it is possible that samples obtained in the earlier work contained a product or products from decomposition of the 1:1 compound as suggested by the studies of Goubeau. Attempts to obtain the mass spectrum of the 1:1 compound by FAB-MS analysis methods were unsuccessful. Ions due to $(\text{MeO})_3\text{B}$ and NH_3 were observed, but none corresponding to a parent ion $(\text{MeO})_3\text{B}\cdot\text{NH}_3^+$ or its expected fragments were detected. However, a chemi-ionization (CI) mass spectrum was recorded using isobutane, and it showed the presence of ions ($M + \text{C}_4\text{H}_8^+$), ($M + \text{C}_4\text{H}_7^+$), ($M + \text{H}^+$), and (M^+). The observation of these ions using this soft ionization method is consistent with the existence of a weakly bound 1:1 complex, $(\text{MeO})_3\text{B}\cdot\text{NH}_3$, in the gas phase at 23 °C above solid samples of the 1:1 compound.

Since the analytical and spectroscopic data do not provide unambiguous characterization of the unusual 1:1 complex, single-crystal X-ray diffraction analysis was performed. A view of the molecule is shown in Figure 1, and a partial view of the unit cell showing hydrogen-bonding interactions appears in Figure 2. Selected bond lengths and angles are

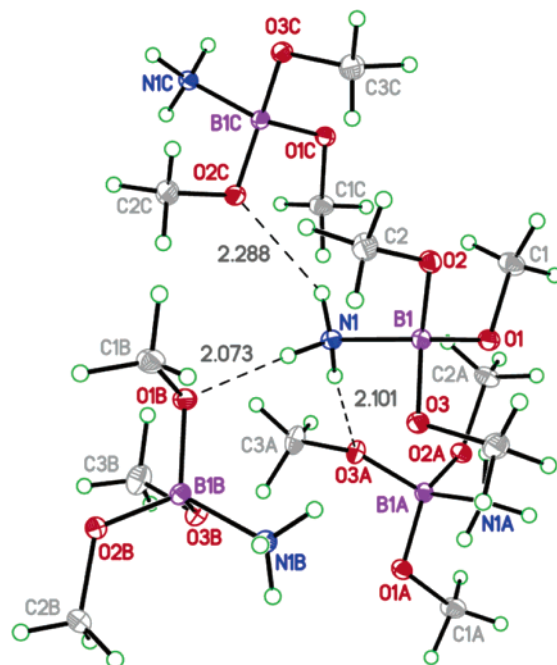


Figure 2. Hydrogen-bonding interactions between $(\text{MeO})_3\text{B}\cdot\text{NH}_3$ molecular units.

Table 2. Selected Bond Lengths (Å) and Angles (deg)

O(1)–C(1)	1.4099(18)	O(1)–B(1)	1.4501(17)
O(2)–C(2)	1.4151(16)	O(2)–B(1)	1.4487(17)
O(3)–C(3)	1.4132(18)	O(3)–B(1)	1.4526(17)
N(1)–B(1)	1.6243(16)		
C(1)–O(1)–B(1)	118.00(11)	C(2)–O(2)–B(1)	117.54(11)
C(3)–O(3)–B(1)	115.16(11)	O(2)–B(1)–O(1)	109.12(10)
O(2)–B(1)–O(3)	115.31(11)	O(1)–B(1)–O(3)	110.15(10)
O(2)–B(1)–N(1)	111.40(10)	O(1)–B(1)–N(1)	109.11(10)
O(3)–B(1)–N(1)	101.45(10)		

summarized in Table 2. The molecular unit is the 1:1 adduct, $(\text{MeO})_3\text{B}\cdot\text{NH}_3$, in which the B and N atoms have a pseudo-tetrahedral geometry. The ammonia fragment is little modified from its resting state structure; however, the borate is distorted from its base-free planar configuration.²⁹ The B–N bond length, 1.624(2) Å, is comparable to the B–N bond length in $\text{F}_3\text{B}\cdot\text{NH}_3$, 1.60(2) Å,³⁰ but it is longer than the B–N bond lengths observed in crystal structure determinations for $\text{Cl}_3\text{B}\cdot\text{NH}_3$ (1.579(4) Å)³¹ and $\text{H}_3\text{B}\cdot\text{NH}_3$ (1.564(6) Å).³² The molecular structures of $\text{F}_3\text{B}\cdot\text{NH}_3$ ³³ and $\text{H}_3\text{B}\cdot\text{NH}_3$ ³⁴ have also been determined by microwave spectroscopy, and in both cases the B–N bond length is significantly longer in the gas phase, 1.67(1) and 1.66(2) Å, respectively. The shorter distances in the solid-state structures have been suggested to arise in response to intermolecular dipole–dipole attractions.^{32,33} The average B–O bond length in the 1:1 complex, 1.451(2) Å, is significantly longer than the B–O bond length

(27) Sallay, S. I. U.S. Patent 4,382,025, May 3, 1983.

(28) Sallay²⁷ reported that the ^1H NMR spectrum of $(\text{MeO})_3\text{B}\cdot\text{NH}_3$ in CDCl_3 shows two resonances at δ 3.50 and 1.45 in an area ratio of 3:1 that were assigned to OCH₃ and N–H groups. Sallay also reported an IR spectrum for the compound claimed to be $(\text{MeO})_3\text{B}\cdot\text{NH}_3$ in Nujol oil with absorptions at 2900, 2840, 2210, 1970, 1450, 1370, 1340, 1200, 1050, 960, and 920 cm^{-1} . Given the properties of $(\text{MeO})_3\text{B}\cdot\text{NH}_3$ observed in our study, it is unlikely that these spectroscopic data are representative of $(\text{MeO})_3\text{B}\cdot\text{NH}_3$. It is possible that the data result from one or more degradation products or an ammonium borate.

(29) Beach, J. Y.; Bauer, S. H. *J. Am. Chem. Soc.* **1941**, *63*, 1394.

(30) Hoard, J. L.; Geller, S.; Cashin, W. M. *Acta Crystallogr.* **1951**, *4*, 396.

(31) Avent, A. G.; Hitchcock, P. B.; Lappert, M. F.; Liu, D.-S.; Mignani, G.; Richard, C.; Roche, E. *J. Chem. Soc., Chem. Commun.* **1995**, 855.

(32) Bühl, M.; Steinke, T.; v. R. Schleyer, P.; Boese, R. *Angew. Chem., Int. Ed.* **1991**, *30*, 1160. The structure determination for $\text{H}_3\text{B}\cdot\text{NH}_3$ was originally performed on powder diffraction data: Hughes, E. W. *J. Am. Chem. Soc.* **1956**, *78*, 503.

(33) Fujiang, D.; Fowler, P. W.; Legon, A. C. *J. Chem. Soc., Chem. Commun.* **1995**, 113.

(34) Thorne, L. R.; Sueniam, R. D.; Lovos, F. J. *J. Chem. Phys.* **1983**, *78*, 167.

reported from the early electron diffraction analysis of $(\text{MeO})_3\text{B}$, 1.38(2) Å.²⁹ This is consistent with distortion of the boron atom from a planar geometry in the base-free acceptor to the pseudo-tetrahedral geometry in the complex. The bond lengthening is accompanied by O–B–O bond angle compression (avg. O–B–O, 111.5°).

Several structures containing $\text{B}(\text{OMe})_4^-$ have been reported,^{35–39} and it is appropriate to compare the structural features in the complex with those in the anion. Interestingly, all of the structures containing $\text{B}(\text{OMe})_4^-$ show a tetragonally distorted pseudo-tetrahedral anion geometry. In all but one case the distortion may at first be considered to result from intermolecular interactions or cation coordination to one or more oxygen atoms. However, in one case, benzyltrimethylammonium tetramethoxyborate,³⁹ there appears to be no significant intermolecular or interionic interactions, indicating that the distortion is intrinsic to the anion. The ranges of B–O and O–C bond lengths in the anion are 1.461(3)–1.473(3) and 1.394(3)–1.417(3) Å, respectively. Four bond angles are similar, from 112.4(2)° to 113.9(2)°, and greater than ideal, while two, 101.2(2)° and 102.9(2)°, are smaller. The average B–O bond length in the complex, 1.451(2) Å, falls at the low end of all distances reported for the tetramethoxyborate ion, 1.451–1.482 Å, while the O–C bond length in the complex is in the middle of the range, 1.391–1.443 Å, observed for $\text{B}(\text{OMe})_4^-$. The bond angles about the central boron atom are also distorted from ideal tetrahedral, and the largest distortions involve the B(1)–O(3) bond vector: N(1)–B(1)–O(3) = 101.45° and O(2)–B(1)–O(3) = 115.31°.

An additional interesting feature in the structure of $(\text{MeO})_3\text{B}\cdot\text{NH}_3$ appears when the intermolecular interactions in the unit cell are examined. The structure contains eight molecules in the unit cell, and the monomeric molecular units are associated with each other through N–H···O–B hydrogen bonds that involve each NH_3 hydrogen atom and each $(\text{MeO})_3\text{B}$ oxygen atom. The H···O distances fall in the range 2.063–2.288 Å. It is likely that the extensive network of hydrogen bonds is largely responsible for the stabilization of the complex in the solid state. If this is the case, it is not surprising that the complex readily dissociates when combined with common organic solvents prior to NMR analysis and fails to produce a parent ion in electron impact mass spectrometric analysis. Indeed, based upon the B–N bond length elongations going from solid-state structures to gas-phase structures for $\text{F}_3\text{B}\cdot\text{NH}_3$ and $\text{H}_3\text{B}\cdot\text{NH}_3$, it might be estimated that the B–N bond length in a putative gas-phase molecule $(\text{MeO})_3\text{B}\cdot\text{NH}_3$ would be ~1.69–1.72 Å, which is outside the normal range of B–N single-bond distances. It is also worth noting that the unit cell of $(\text{MeO})_3\text{B}\cdot\text{NH}_3$ reveals channels extending along the *c* axis. It is tempting to suggest that these channels may loosely accommodate

excess ammonia over the 1:1 complex stoichiometry through intermolecular hydrogen bonding, which would be consistent with the qualitative observation that the solid complex appears to reversibly absorb and desorb ammonia.

The thermal stability of $(\text{MeO})_3\text{B}$ up to at least 400 °C in the absence of NH_3 , the relatively weak donor–acceptor interaction between $(\text{MeO})_3\text{B}$ and NH_3 at room temperature, and the observed elimination of MeOH and Me₂O from mixtures of $(\text{MeO})_3\text{B}$ and NH_3 above room temperature suggest that the elimination chemistry first observed by Schechter,²⁰ Goubeau,^{21–23} and May²⁴ is intermolecular in nature and the reagents should be useful as precursors in an aerosol reactor synthesis of BN.⁴⁰

In the aerosol powder synthesis the nitridation of $(\text{MeO})_3\text{B}$ aerosols in NH_3/N_2 gas mixtures is performed in two stages due to the relatively short particle residence time in the reactor flight tube. The first stage involves generation of aerosol droplets of neat $(\text{MeO})_3\text{B}$ that are transported in a nitrogen gas stream from the aerosol generator into a horizontal pyrolysis flight tube.^{12,14} Ammonia gas is separately injected into the reaction zone, and the pyrolysis product, $\text{BN}_x\text{O}_y\text{C}_z$,⁴¹ a white to cream colored solid, is collected on an impact or a bag filter at the exit end of the reactor flight tube. The primary experimental reactor variables studied were temperature, total gas flow rate, and the NH_3/N_2 flow rate ratio. These factors are found to dramatically impact the composition of powders and their subsequent nitridation performance. Under the conditions reported here, the reactor provides 95–100% recovery of boron as $\text{BN}_x\text{O}_y\text{C}_z$ based upon $(\text{MeO})_3\text{B}$ injected into the reactor.⁴² This conversion is superior to the $\text{H}_3\text{BO}_3/\text{H}_2\text{O}/\text{NH}_3$ aerosol system¹³ where the solid products contain a significant

(35) Zachariasen, W. H. *Acta Crystallogr.* **1963**, *16*, 385.

(36) Heller, G.; Horbat, F. Z. *Naturforsch.* **1977**, *32b*, 989.

(37) Alcock, N. W.; Hagger, R. M.; Harrison, W. D.; Wallbridge, M. G. *Acta Crystallogr.* **1982**, *B38*, 676.

(38) Al-Juaid, S. S.; Eaborn, C.; El-Kheli, M. N. A.; Hitchcock, P. B.; Lickiss, P. D.; Molla, M. E.; Smith, J. D.; Zora, J. A. *J. Chem. Soc., Dalton Trans.* **1989**, 447.

(39) Clegg, W.; Errington, R. J.; Carmalt, C. J. *Acta Crystallogr.* **1977**, *C53*, 751.

(40) Although no effort was made to obtain reaction kinetic data for the $(\text{MeO})_3\text{B}/\text{NH}_3$ system or deduce the details of the mechanism of substituent group elimination, the general features of the elimination chemistry reported in part by Goubeau^{21–23} and May and Levasheff²⁴ have been confirmed. In static reaction containers, solid samples of the 1:1 complex are clearly in equilibrium with $(\text{MeO})_3\text{B}$ and NH_3 at 23 °C as noted in the text. Solid samples of the complex have been stored in sealed containers for >2 years at 23 °C with no sign of decomposition via elimination. At temperatures above 200 °C gas-phase mixtures of $(\text{MeO})_3\text{B}$ and NH_3 very slowly deposit a white solid, and above 400 °C the solid deposition appears over days along with measurable MeOH formation. In a flowing gas reactor tube held at 600 °C, $(\text{MeO})_3\text{B}$ and NH_3 typically pass through the reactor without significant conversion and are recovered as the adduct following condensation in a cold trap at the reactor exit. The lack of conversion is probably due to a short residence time in the reactor hot zone where the gases may not reach the set temperature of the tube. Above this temperature a white solid deposits on the cold walls of the tube outside the hot zone. This is consistent with the aerosol process described here and the CVD studies of Bando and co-workers.²⁶ These results and the aerosol transformation chemistry appear to be most consistent with facile intermolecular substituent group elimination processes starting with $(\text{MeO})_3\text{B}$ and NH_3 as opposed to intramolecular eliminations originating from the weak adduct $(\text{MeO})_3\text{B}\cdot\text{NH}_3$.

(41) The solid products harvested from the aerosol reactor are generally referred to as $\text{BN}_x\text{O}_y\text{C}_z$ where *x*, *y*, and *z* vary depending upon reactor process parameters. These products contain small amounts of hydrogen as well. These products are also referred to as stage 1 products and are the solid-state precursor for stage 2 calcinations that produce BN containing low levels of O, C, and H impurities.

(42) In a typical experimental run at 1400 °C with N_2 flow rate (2 L/min) and NH_3 flow rate (3 L/min) held constant, ~18.6 g of $(\text{MeO})_3\text{B}$ aerosol was injected over 15 min into the reactor and ~4.3 g of $\text{BN}_x\text{O}_y\text{C}_z$ powder was recovered on the impact filter. On the basis of the elemental analysis of the product, this corresponds to ~97% recovery of boron.

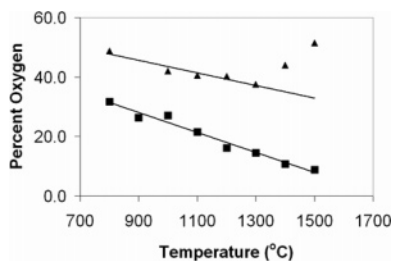


Figure 3. Variation of oxygen content (wt %) in $\text{BN}_x\text{O}_y\text{C}_z$ (■) and BN_xO_y (▲) aerosol samples as a function of process temperature with gas flow rates $\text{N}_2 = 1$ L/min and $\text{NH}_3 = 3$ L/min.

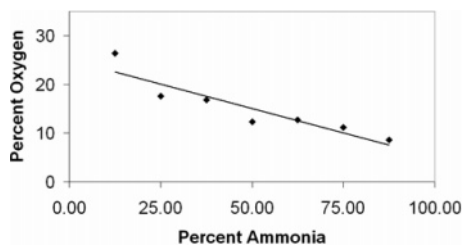


Figure 4. Variation of oxygen content (wt %) in $\text{BN}_x\text{O}_y\text{C}_z$ aerosol samples as a function of NH_3 concentration (% NH_3 in N_2) in process gas stream at 1400 °C.

amount of B_2O_3 under some process conditions, some of which escapes without nitridation. Depending upon temperature and flow rate in the $(\text{MeO})_3\text{B}/\text{NH}_3$ system, the production rate of collected powder is 0.1–1 g/min, which is 50–100 times the rate of formation of the BN_xO_y precursor from the boric acid system.

The improved conversion efficiency in the $(\text{MeO})_3\text{B}/\text{NH}_3$ system is revealed in plots of $\text{BN}_x\text{O}_y\text{C}_z$, wt % oxygen composition vs reactor temperature. A typical plot (Figure 3) for the $(\text{MeO})_3\text{B}/\text{NH}_3$ system (■) for the flow rates $\text{N}_2 = 1$ L/min and $\text{NH}_3 = 3$ L/min⁴³ show a steady decrease in the wt % oxygen content with increasing temperature of the reactor tube. Similar graphs are obtained using a range of N_2/NH_3 ratios (1/7 to 7/1), total flow rates (1 to 8 L/min), and reactor tube temperatures (800–1500 °C) that result in estimated aerosol particle residence times in the reactor between 120 and 10 s. It is also noted that at a fixed temperature, wt % oxygen contents in the $\text{BN}_x\text{O}_y\text{C}_z$ powders steadily decrease as the gas mixture becomes richer in NH_3 . This is illustrated in Figure 4 for a series of powders collected at 1400 °C with a total flow rate of $\text{N}_2 + \text{NH}_3 = 4$ L/min.

As noted above, the conversion performance in the $(\text{MeO})_3\text{B}/\text{NH}_3$ system is superior to that in the $\text{H}_3\text{BO}_3/\text{H}_2\text{O}/\text{NH}_3$ system. Not only is the powder production rate much higher in the $(\text{MeO})_3\text{B}/\text{NH}_3$ system, but the absence of water in the aerosol and in the borate decomposition/nitridation chemistry eliminates the deleterious high-temperature back-reaction of steam with the formation of $\text{BN}_x\text{O}_y\text{C}_z$ particles. The lower oxygen content signifies greater conversion to BN in the first-stage process. The onset of the back-reaction in the $\text{H}_3\text{BO}_3/\text{H}_2\text{O}/\text{NH}_3$ system (▲) at 1300–1400 °C is illustrated in Figure 3. Under all conditions studied, the

amount of oxygen in the $\text{BN}_x\text{O}_y\text{C}_z$ powders is significantly less than that in the BN_xO_y powders.

The $\text{BN}_x\text{O}_y\text{C}_z$ stage-one powders were characterized by thermal gravimetric analysis (TGA), oxygen elemental analysis, density, surface area determinations, diffuse reflectance FT-IR, powder X-ray diffraction (XRD), and scanning electron microscopy (SEM). In some cases, full elemental analysis data (B, N, C, H) were obtained as well. As indicated in Figures 3 and 4, the $\text{BN}_x\text{O}_y\text{C}_z$ powders typically show oxygen contents in the range 8–36 wt %. For samples with full analyses, the following ranges were observed: B, 32–41 wt %; N, 32–46 wt %; C, 0.2–1.1 wt %; H, 0.5–2.0 wt %.⁴⁴ As expected, higher reactor temperatures give lower wt % values for O, C, and H and higher wt % values for B and N. The density of powders range from 1.55 to 2.1 g/cm³ compared with the values of 2.20 g/cm³ for pure h-BN and 1.80 g/cm³ for B_2O_3 . In general, the powder density increases with increasing reactor temperature and increasing mole fraction of NH_3 in the gas process stream. The DRIFT-IR spectra for $\text{BN}_x\text{O}_y\text{C}_z$ powders show a broad, very strong absorption centered at 1410 cm⁻¹, a sharp, medium intensity band at 808 cm⁻¹, and a broad very weak absorption spanning the region 3500–3200 cm⁻¹. The lower frequency band pattern is very similar to that displayed in the spectrum by h-BN samples¹ (~1370 and ~810 cm⁻¹); however, the breadth and up-frequency shift of the strong band at 1410 cm⁻¹ and the weak band at 3500–3200 cm⁻¹ are consistent with the presence of B–O and O–H bonds resulting from incomplete nitridation and/or adsorbed water. Powder XRD scans for the samples, in all cases, show two moderately broad reflections centered at $2\theta = 24.7^\circ$ and 43.2° . These scans are similar although of greater intensity than those reported for the BN_xO_y powders obtained in the $\text{H}_3\text{BO}_3/\text{H}_2\text{O}/\text{NH}_3$ aerosol system.¹² Scanning electron microscopy analysis of the $\text{BN}_x\text{O}_y\text{C}_z$ powders shows the formation of smooth, spherically shaped particles with diameters in the range 0.2–2 μm. A typical micrograph is shown in Figure 5. In many samples the SEM micrographs show that there is a greater degree of primary particle agglomeration than observed with either the aqueous $\text{H}_3\text{BO}_3/\text{NH}_3$ ¹² or the aqueous guanidinium borate/ NH_3 ¹⁴ systems. This is very likely an outcome of the high concentration of boron precursor in the $(\text{MeO})_3\text{B}/\text{NH}_3$ system.

Although the process described above for formation of $\text{BN}_x\text{O}_y\text{C}_z$ particles is superior in production rate and oxygen content compared to the aqueous $\text{H}_3\text{BO}_3/\text{NH}_3$ system, a second-stage pyrolysis is still required in order to obtain BN particles having low oxygen and carbon contents. Prior to examining the second-stage nitridations of $\text{BN}_x\text{O}_y\text{C}_z$ particles, the materials were examined by thermal gravimetric analysis. Typical scans obtained with nitrogen purge (40 mL/min) are shown in Figure 6 for $\text{BN}_x\text{O}_y\text{C}_z$ samples prepared at 1100, 1300, and 1500 °C ($\text{N}_2 = 1$ L/min, $\text{NH}_3 = 3$ L/min). The 1100 °C material shows two weight-loss events in the ranges

(43) The flow rates quoted in this study correspond to gas flow rates (N_2 and NH_3) at the front of the reactor. The effective total flow rate in the hot zone and hence the particle residence time is influenced by the decomposition and reaction of NH_3 and formation of gaseous byproducts, e.g., MeOH in the reactor.

(44) As examples, the analysis of a $\text{BN}_x\text{O}_y\text{C}_z$ sample prepared at 1400 °C with gas flow rates $\text{N}_2 = 1$ L/min and $\text{NH}_3 = 3$ L/min gave B 41.11, C 0.89, H 1.08, N 45.12, O 8.3, and the analysis of a sample prepared at 1000 °C with gas flow rates $\text{N}_2 = 0.5$ L/min and $\text{NH}_3 = 0.5$ L/min gave B 27.24, C 0.59, H 1.22, N 35.61, O 22.6.

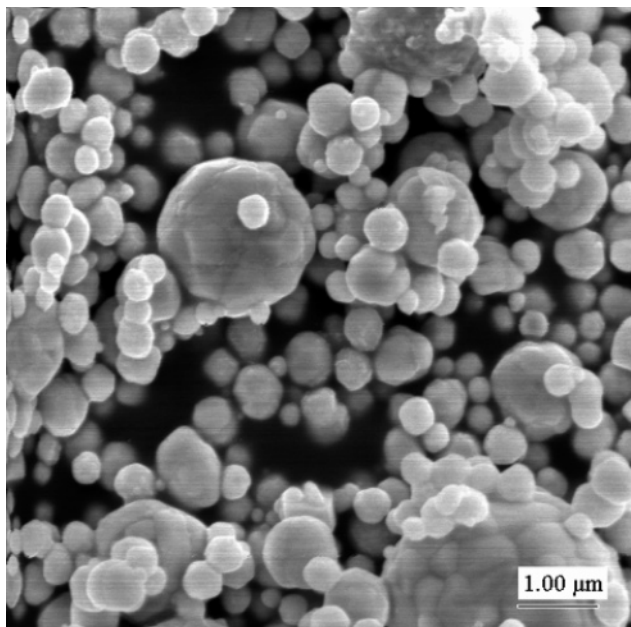


Figure 5. SEM image of $\text{BN}_x\text{O}_y\text{C}_z$ powder sample obtained at 1400 °C.

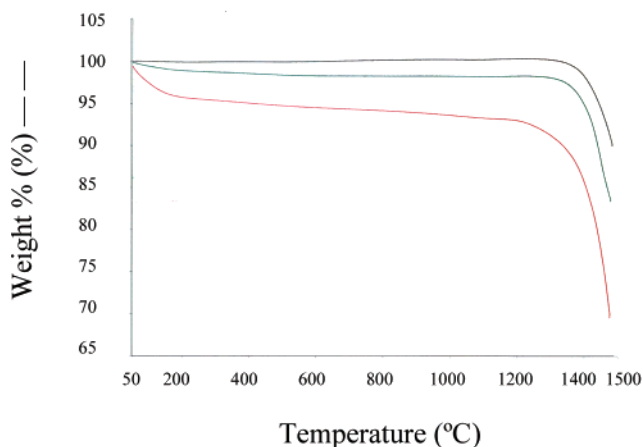


Figure 6. TGA traces for $\text{BN}_x\text{O}_y\text{C}_z$ powders prepared at 1100 (red), 1300 (green), and 1500 °C (black). Traces recorded under nitrogen purge (50 mL/min; 40 °C/min).

50–200 (~4%) and 1200–1450 °C (~25%). It is assumed that the first event corresponds to dehydration of H_3BO_3 present as a low-level impurity or perhaps methanol loss from an incompletely converted boron oxide methoxide species while the second event probably results from volatilization of borate trapped in the solid. In fact, a TGA scan for H_3BO_3 shows two weight-loss events in the ranges 50–210 (42%) and 1150–1400 °C (45%). The first is due to dehydration, and the second corresponds to B_2O_3 volatilization. It is obvious that both losses are greatly reduced in the 1300 and 1500 °C materials, which is consistent with a greater degree of starting material transformation/nitridation and concomitant reduced oxygen contents in the $\text{BN}_x\text{O}_y\text{C}_z$ aerosol samples formed at higher pyrolysis temperatures.

The TGA of a $\text{BN}_x\text{O}_y\text{C}_z$ sample obtained at 1100 °C was also recorded under an NH_3 purge (20 mL/min of NH_3 + 30 L/min of N_2), and that trace is shown in Figure 7 overlaid on the trace obtained under N_2 purge. The initial weight-loss event (50–200 °C) in the two samples is essentially identical, but the remaining behavior is quite

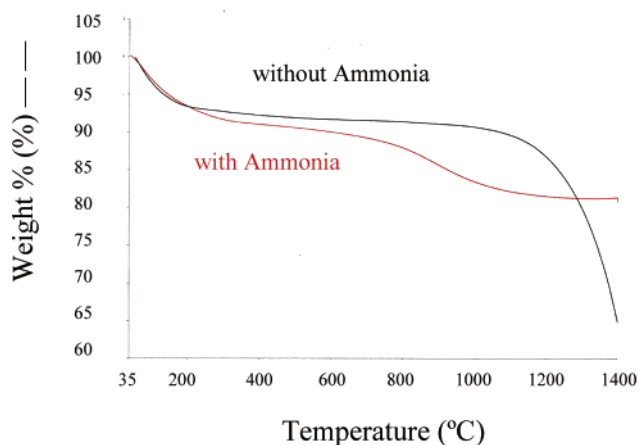


Figure 7. TGA traces for $\text{BN}_x\text{O}_y\text{C}_z$ powders prepared at 1100 °C under N_2 (red) and NH_3 (black) purge (30 L/min + 20 mL/min; 40 °C/min).

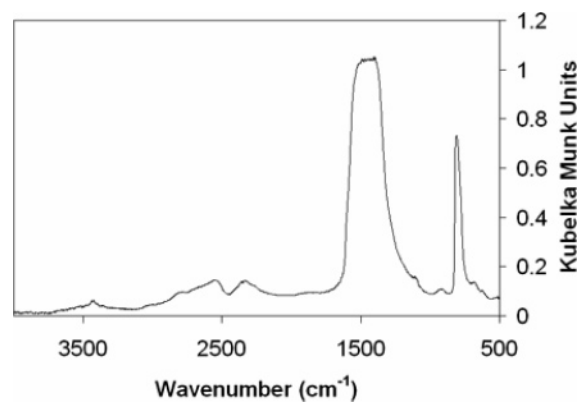


Figure 8. DRIFT-IR spectrum for BN aerosol particles obtained from nitridations of $\text{BN}_x\text{O}_y\text{C}_z$ at 1600 °C under NH_3 (0.5 L/min).

different. Most importantly, the dramatic weight loss above 1200 °C is absent when ammonia is present since nitridation instead of B_2O_3 volatilization is taking place.

On the basis of these findings second-stage nitridations of $\text{BN}_x\text{O}_y\text{C}_z$ samples were undertaken. Samples were placed in a boron nitride crucible, and the samples were heated to 1200–1600 °C under a slow purge of NH_3 (0.5 L/min). The same general results are obtained in each case, but the rate of transformation is faster at higher temperatures. Characterization data presented here are for samples nitrided at 1600 °C. Elemental analyses show nearly complete nitridation/conversion to BN with O, C, and H contents less than 1 wt %.⁴⁵ The macroscopic weight losses during nitridations are 10–25 wt %, in agreement with the TGA data. The densities of the powders fall in the narrow range of 2.0–2.2 g/cm³, and the BET surface areas are typically 5–15 m²/g. The DRIFT-IR spectra (Figure 8) of nitrided samples show a very strong band centered at 1467 cm⁻¹ that is sharper than this absorption in the precursor $\text{BN}_x\text{O}_y\text{C}_z$ material. In addition, a sharp characteristic absorption centered at 811 cm⁻¹ is present and the weak, high-frequency band in the region 3500–3200 cm⁻¹ is absent, supporting the conversion of unreacted B–O–H and B–N–H bonds. The powder XRD

(45) As an example, the analysis of a second-stage sample, obtained from calcination of stage 1 sample prepared at 1400 °C, gave B 43.68, C 0.60, H 0.96, N 55.69, O 0.73. This sample displayed a measured 14.5% mass loss.

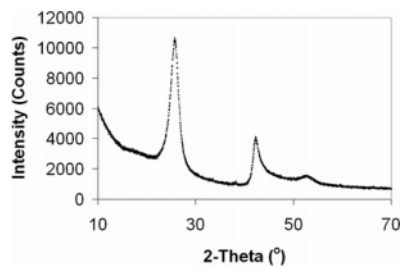


Figure 9. Powder XRD scan for BN aerosol particles obtained from nitridations of $\text{BN}_x\text{O}_y\text{C}_z$ at 1600 °C under NH_3 (0.5 L/min).

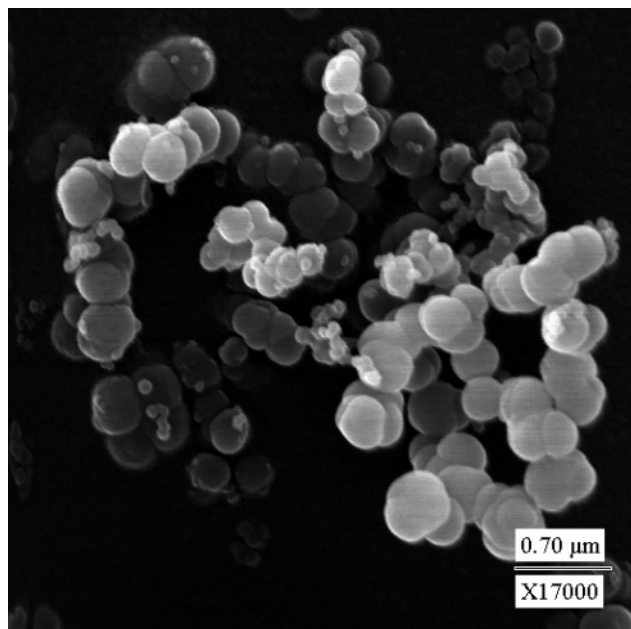


Figure 10. SEM image of BN particles from nitridations of $\text{BN}_x\text{O}_y\text{C}_z$ at 1600 °C.

pattern (Figure 9) is sharpened, relative to the $\text{BN}_x\text{O}_y\text{C}_z$ precursor ($2\theta = 25.7^\circ$ and 42.3°), but is still indicative of turbostratic BN. The SEM micrographs (Figure 10) of the BN particles show that the particles retain the general size and spherical morphology of the $\text{BN}_x\text{O}_y\text{C}_z$ particles shown in Figure 5. A transmission electron micrograph (TEM) (Figure 11) shows that the particles develop a “crumpled aluminum foil ball” surface structure that is different from the very smooth surface nanostructure reported in our earlier work on the aqueous $\text{H}_3\text{BO}_3/\text{NH}_3$ system.¹²

Given the very high production rates and low oxygen levels for $\text{BN}_x\text{O}_y\text{C}_z$ powders produced in the solventless $(\text{MeO})_3\text{B}/\text{NH}_3$ system and the subsequent facile, high-yield conversion to spherical BN particles, this process represents a very significant advancement for the production of these unique particles. Nonetheless, the observation that some samples show particle agglomeration led us to examine several additional modifications on this system. In one modification the use of $(\text{EtO})_3\text{B}$, $(n\text{-PrO})_3\text{B}$, and $(n\text{-BuO})_3\text{B}$ as the boron starting material was examined. It was initially thought that the increased organic carbon present in the alkyl groups would deposit additional carbon in the first-stage aerosol $\text{BN}_x\text{O}_y\text{C}_z$ powders and further facilitate carbothermal reduction/nitridation in the second stage. Indeed, these systems generate $\text{BN}_x\text{O}_y\text{C}_z$ materials having higher carbon contents ($>10\%$), but the agglomeration issue is not improved and the nitridation rate is not dramatically improved.

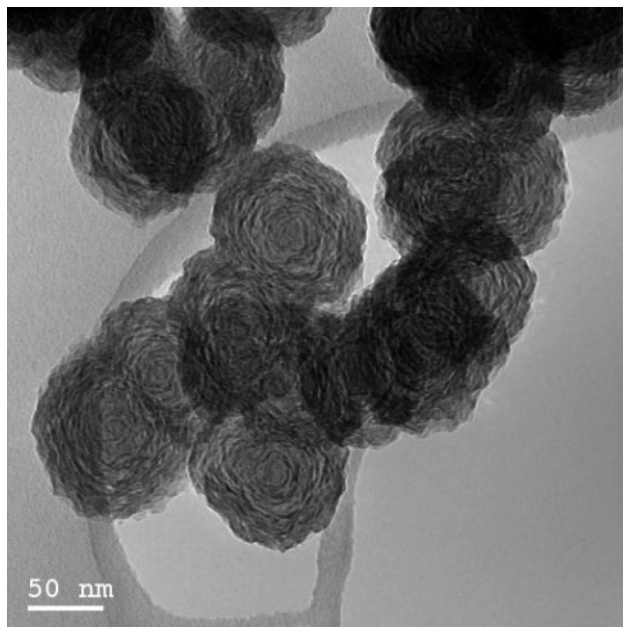


Figure 11. TEM image of BN particles from nitridations of $\text{BN}_x\text{O}_y\text{C}_z$ at 1600 °C.

As a result, these precursors do not offer a practical improvement over $(\text{MeO})_3\text{B}$. In another approach an azeotropic mixture (70%) of $(\text{MeO})_3\text{B}$ in MeOH was examined as a starting aerosol solution. The mixture forms a useful aerosol, and pyrolysis at 1000 ($\text{N}_2 = 0.5$ L/min, $\text{NH}_3 = 3.5$ L/min) and 1400 °C ($\text{N}_2 = 0.5$ L/min, $\text{NH}_3 = 3.5$ L/min) gave tan and white powders with oxygen contents of 18.6 and 9.8 wt %, respectively. Subsequent calcinations at 1600 °C under NH_3 gave white solids with oxygen contents of 0.8 and 0.9 wt %, respectively. The SEM micrographs for these solids show the presence of lightly agglomerated BN particles much like those shown in Figure 10.

It is known that mixtures of H_3BO_3 or B_2O_3 in MeOH produce $(\text{MeO})_3\text{B}$ when heated.¹⁷ Since these boron reagents are less expensive than commercially prepared, reagent-grade $(\text{MeO})_3\text{B}$, MeOH solutions of H_3BO_3 (8:1) and B_2O_3 (12:1) were explored as feedstocks. These solutions form aerosol streams, and each produces flowing cream to white colored $\text{BN}_x\text{O}_y\text{C}_z$ aerosol powders at 1000 and 1400 °C ($\text{N}_2 = 0.5$ L/min, $\text{NH}_3 = 3.5$ L/min). Analyses for these samples give oxygen contents in the range 20–25%, comparable to the oxygen contents in the $\text{BN}_x\text{O}_y\text{C}_z$ solids obtained from neat $(\text{MeO})_3\text{B}$ aerosols. SEM analyses show that the powders are composed of unagglomerated spheres in the size range 0.5–2 μm typically “dusted” with fine particles. The fine particles likely result from violent fracture of hollow particles formed in the process. Subsequent second-stage nitridations at 1600 °C give BN samples with oxygen contents of 0.8–1.6 wt %. These products are no longer free flowing but are obtained as a sintered mass that must be ground for subsequent XRD and SEM analyses. Powder XRD analysis provides evidence for formation of turbostratic BN. The SEM analyses show spherical particles embedded in “webs” of BN. The resulting surface areas for these materials (30–70 m^2/g) are approximately 10 times greater than those found for the neat $(\text{MeO})_3\text{B}$ aerosol materials and the densities, 1.5–1.6 g/cm^3 , are reduced from the materials obtained from neat borate.

These powders may prove useful for future applications, but they are not attractive for use as dense filler particles in organic polymer composites.

In conclusion, this study shows that neat trimethyl borate, $(\text{MeO})_3\text{B}$, serves as a good aerosol feedstock when combined with NH_3 for the formation of spherical morphology $\text{BN}_x\text{O}_y\text{C}_z$ solid-state materials that can be easily converted in second-stage nitridations under ammonia to spherical morphology BN particles that are lightly agglomerated. These powders contain low levels of oxygen and carbon impurities comparable to the highest grade platelet-shaped particles prepared in industrial manufacturing processes. The study also suggests related approaches for one-stage aerosol production of BN without the second-stage nitridation. The process is efficient, showing low loss of boron during the two-step

process. Further studies of this system incorporating additive combinations that produce ceramic composite materials are in progress.

Acknowledgment. Financial support for this study was provided by the National Science Foundation (CHE-9983205). This includes support for an international U.S.–Poland collaboration (R.T.P./J.F.J.).

Supporting Information Available: Full unit cell view of the complex $(\text{MeO})_3\text{B}\cdot\text{NH}_3$, and additional IR and XRD data for $\text{BN}_x\text{O}_y\text{C}_z$ powders and SEM micrographs of $\text{B}_2\text{O}_3/\text{MeOH}$ 1:12 aerosol powder obtained at 1000 °C and calcined at 1600 °C. This material is available free of charge via the Internet at <http://pubs.acs.org>.

CM052032X